Chapter 3

Cyclic behavior of soil and interrelationships among parameters involved

3.1 Introduction

Repetitive passages have been reported as a major cause of aggravating the incidence of field soil compaction[85]. Many efforts have been made to reduce the adverse effect of soil compaction. One of the most important concerns regarding soil compaction is to investigate the process of soil compaction and the its behavior while being subjected to an external force system induced by machinery traffic.

During the passage of a vehicular machine in the field, the loads transmitted to the soil element are dynamic in terms of both magnitude and direction. As for these actual phenomena, it implies that the conventional static triaxial compression test which is usually used for solving the problem of static soil compaction seems to be inadequate to help explain the behavior of the soil compacting process under such phenomena. This is because of some intrinsic limitation of the test methods in relation to the rate of loading as mentioned by Karafiath and Nowatziki[47]. Therefore, to clarify such soil compaction in the field, especially on torsional shear deformation, the relevant experimental combinations were provided. The method of cyclic torsional shear loading test, which is usually used in the field of civil engineering, was adopted in a way that can provide the explanation for the specific phenomena of soil compaction described above.

The aim of this study is to clarify the dynamic behaviors of soil compaction under repetitive passages, including the turning operation mode, of a tractor in the field. The parasitic interrelationships among various parameters, including torsional shear stress and

strain, confining stress, loading frequency, bulk density, and number of cyclic loading are also discussed.

3.2 Methodology

3.2.1 Material

The soil used in the experiments was Ishioka sandy loam, which has the physical properties listed in Table 3.1. This soil was sampled in the paddy field at Ishioka, Ibaraki Prefecture, Japan. It is a low-land soil having a medium fine particle and gray in color[46]. The reason for the selection of this soil being used in this test is that it is a paddy soil and dominates elsewhere in this area. Another consideration is that this soil type is intermediate between sand and clay. For sand, this type of test has been widely conducted in the field of civil engineering and it is not recognized as a paddy soil. On the other hand, for clay soil, it is very complicated to conduct the test and clarify its behavior. Therefore, for the first stage of the study, the test soil is adopted for a type intermediate between sand and clay.

Table 3.1 Physical properties of test soil

Soil Type	Specific gravity	Gradation (%)			Liquid limit	Plastic limit
		Sand	Silt	Clay		
Sandy loam	2.64	62.3	25.4	12.3	NP	NP

Note: NP stands for non-plastic characteristics.

Based on the standard system of JIS A 1204 and JSF M1, this soil is categorized as sandy loam type and SM type, respectively. The judgement of non-plastic characteristics came from the fact that in the liquid limit test it was difficult to make a groove and the soil

at the bottom of the groove did not expand, but the sliding of soil on the disk led the groove closer. Also, in the plastic limit test, the soil could not be rolled out into a thin thread of 3 mm in diameter[46]. The particle size distribution curve of this soil is provided in Fig. 3.1.

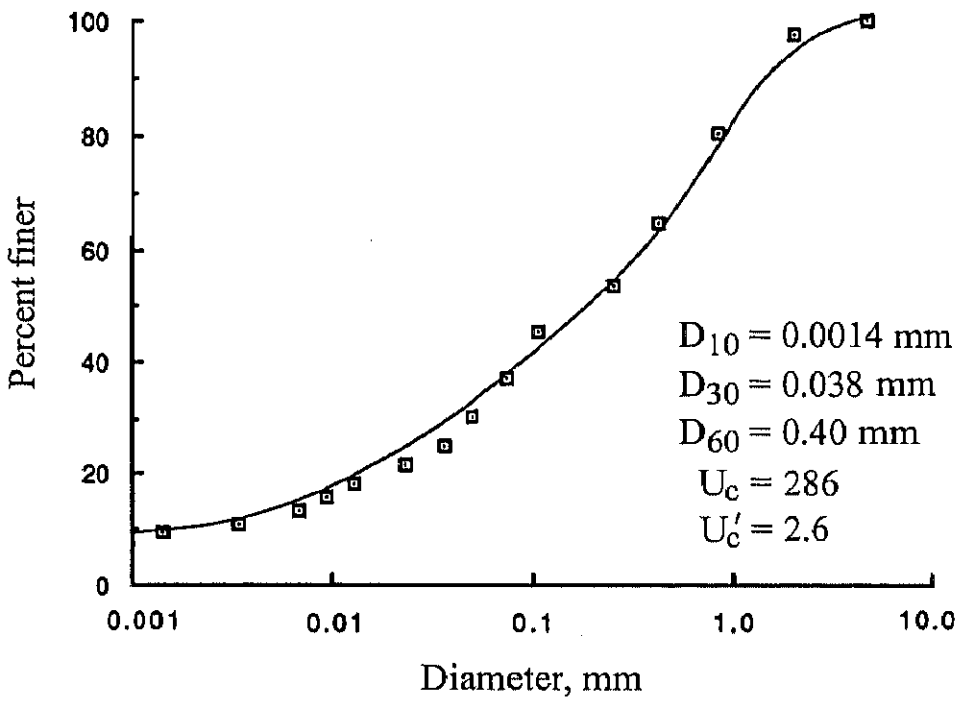

Fig. 3.1 Particle size curve.

3.2.2 Preparation of specimen

Before testing, the soil was air-dried and sieved with 2 mm sieve, and water was added for a moisture content of 25% d.b. This level of moisture content was arbitrarily chosen so as to make the preparation of the soil specimen easy. After the curing process, the soil specimen was made into a hollowed cylindrical shape in order to minimize the problem of different magnitudes of stress along the radial direction of a rigid cylinder. The

size of the soil specimen was 30, 50 and 120 mm in inner radius, outer radius, and height, respectively (Fig. 3.2(a)).

Soil specimens were produced by filling five layers of soil into the space between inner and outer molds. The bulk density of the soil specimen was attained by adjusting the dropping number of a 722.7 g rammer as well as the free fall distance.

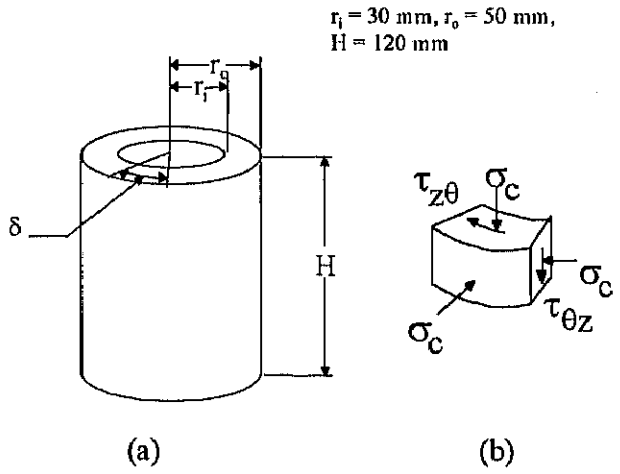

Fig. 3.2 (a) Soil specimen,
(b) stress state on soil element.

With five layers of soil in molds and one and two blows dropped from a distance of 0.03 m to each layer, soil specimens of about 0.9 and 1.0 Mg/m^3 were obtained, respectively. Similarly, one blow and falling distance of 0.02 m brought about the soil specimen of about 0.8 Mg/m^3. These three kinds of soil specimen had void ratios of about 1.93, 1.64 and 2.30, respectively.

3.2.3 Test procedure

After placing the soil specimen on the pedestal, the triaxial chamber was assembled, then the soil specimen was slowly saturated. A high degree of saturation was achieved by applying a back pressure of 200 kPa to the soil specimen during the flow of water through

the specimen. This value of back pressure was recommended by Bishop and Henkel[12] to force scattered small-sized air bubbles to be absorbed by the water. The degree of saturation was confirmed with B value which reached approximately 0.96. The consolidation process was performed at a certain confining stress together with a back pressure of 49 kPa. Afterwards, a constant magnitude of cyclic torsional shear was applied to the specimen and the test was carried out under saturated, undrained condition. The test method adopted here follows the procedure of the cyclic torsional shear loading test standard, or JSF T 543-1994[59].

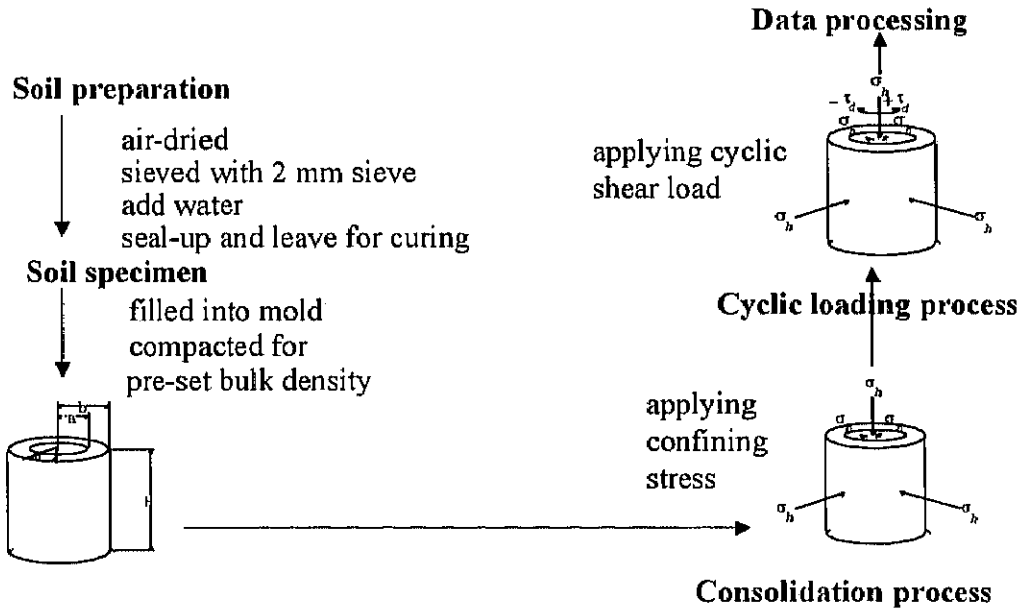

Fig. 3.3 Test procedure.

The test procedure is simply demonstrated in Fig. 3.3. It includes the process of soil preparation, specimen preparation, consolidation, cyclic loading, and data processing.

Great care was taken in the preparation process of the specimen. Some difficulties existed when the inner mold was taken off in an upward direction. However, this was eased

by applying a negative pressure of about 0.2 kPa on the soil specimen. In addition, the placement of a small amount of talcum powder to the inner mold made the removal process easier.

3.2.4 Test apparatus

The cyclic torsional shear loading test apparatus used in this experiment is presented schematically in Fig. 3.4. The major components consist of (1) triaxial chamber, (2) cylinder, (3) motor, (4) water reservoir, (5) air compressor, and (6) vacuum pump. Cyclic torsional movement is produced by a closed-loop servo motor installed above the triaxial chamber. The hydraulic cylinder placed on the top of the device is for adjusting the vertical stress on the soil specimen being constant in anisotropical condition and equal to horizontal stress in isotropical condition during the cyclic torsional shear loading test. This apparatus is also capable of providing cyclic vertical loading with help of a cylinder located above the motor.

A hydrostatic confining pressure was applied to the specimen through water inside the triaxial chamber. It confines both outside and inside faces of the specimen, which are enclosed with rubber membranes. The surfaces of the porous stones of the top cap and the bottom pedestal are fixed with eight stainless blades 1.5 mm high to prevent the specimen from slipping during the test.

Care should also be taken here on placing filter paper on the pedestal. The filter paper should be cut properly and placed firmly on each section of surface. Otherwise some soil particles will be forced into the porous stone of the pedestal and plug the water flow.

For measurement, a two-way load cell measures external axial load and cyclic torsional shear load. A torsional angle pickup and a buret are designed for measuring torsional shear strain and volume of drained water, respectively. Other devices include

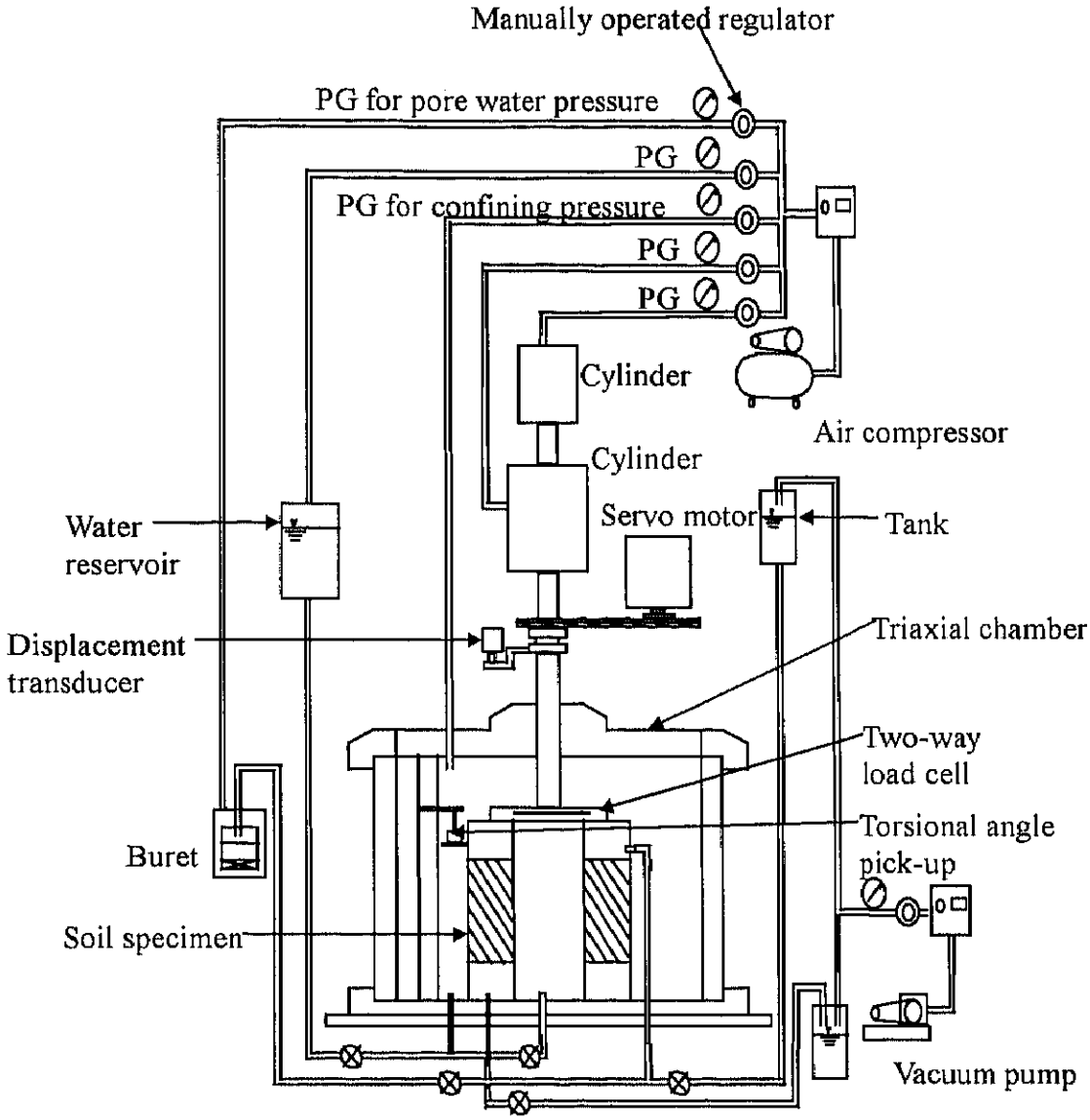

Fig. 3.4 Cyclic torsional shear loading test apparatus.

pressure gauges: a pore water pressure gauge and a confining pressure gauge.

3.2.5 Theoretical description

The stress state that occurred on the soil element under the cyclic torsional shear loading is schematically shown in Fig. 3.2(b). The horizontal and vertical stresses are equal to each other being under the isotropical condition and these stresses can be unified and

referred to as confining stress, σ_c. The cyclic torsional shear stress, $\tau_{z\theta}$, in the figure is calculated from the following equation:

$$\tau_{z\theta} = \frac{3M_T}{2\pi(r_o^3 - r_i^3)} \tag{3.1}$$

where M_T (N·m) is applied torque, r_o (m) is outer radius and r_i (m) is inner radius. Corresponding torsional shear strain, $\gamma_{z\theta}$, is obtainable from:

$$\gamma_{z\theta} = \frac{2\delta(r_o^3 - r_i^3)}{3H(r_o^2 - r_i^2)} \tag{3.2}$$

where δ (rad) is cyclic torsional angle of specimen and H (m) is height of specimen.

Under undrained condition, when the cyclic torsional shear is applied to the soil specimen, the pore water pressure increases. The difference between the magnitude of confining stress and pore water pressure is called the effective confining stress, σ_c', which can be formulated as follows:

$$\sigma_c' = \sigma_c - u_w \tag{3.3}$$

where σ_c (kPa) is confining stress and u_w (kPa) is pore water pressure.

3.2.6 Test combinations

Based on the fact that operation of a tractor in the field produces different loads and different levels of loading frequency transmitted to the soil element, various combinations of test parameters as shown in Table 1 were prepared to help explain the intrinsic effects on the pertinent behavior of soil compaction. Different levels of cyclic torsional shear stresses were provided being suitable to dynamic loads produced by machinery traffic in the field. The loading frequencies were set at 0.2, 0.5 and 1.0 Hz. The reason for choosing these values was described in the concerned section. Moreover, the formation of soil in the field might result in a variety of physical properties depending on its farming practice history.

Therefore, in order to clarify the effect of physical property on the dynamic behavior of soil, the specimens were prepared at three different bulk densities of 0.8, 0.9 and 1.0

Table 3.2 Test combinations

Test No.	Bulk density, Mg/m^3	Frequency, Hz	Cyclic torsional shear stress, kPa	Confining stress, kPa
1	1.01	0.2	6.4	98.0
2	0.99	0.2	10.7	98.0
3	0.98	0.2	14.9	98.0
4	0.98	0.2	17.7	98.0
5	0.99	0.2	19.3	98.0
6	1.01	0.2	21.7	98.0
7	0.99	0.2	23.3	98.0
8	0.91	0.2	6.4	98.0
9	0.92	0.2	10.7	98.0
10	0.90	0.2	14.9	98.0
11	0.91	0.2	17.7	98.0
12	0.90	0.2	19.3	98.0
13	0.80	0.2	6.4	98.0
14	0.81	0.2	10.7	98.0
15	0.83	0.2	14.9	98.0
16	0.83	0.2	17.7	98.0
17	1.00	0.5	6.4	98.0
18	0.97	0.5	10.7	98.0
19	1.01	0.5	14.9	98.0
20	0.99	0.5	17.7	98.0
21	1.00	0.5	19.3	98.0
22	0.98	1.0	6.4	98.0
23	0.98	1.0	10.7	98.0
24	0.99	1.0	14.9	98.0
25	0.98	1.0	17.7	98.0
26	0.98	0.2	10.7	73.5
27	1.01	0.2	10.7	122.5
28	1.01	0.2	10.7	147.0
29	1.01	0.2	10.7	196.0
30	0.99	0.5	10.7	73.5
31	0.98	0.5	10.7	122.5
32	0.99	0.5	10.7	147.0
33	1.01	0.5	10.7	196.0
34	0.82	0.2	10.7	73.5
35	0.83	0.2	10.7	122.5
36	0.83	0.2	10.7	147.0
37	0.82	0.2	10.7	196.0

Mg/m^3 which have void ratios of 2.30, 1.93 and 1.64 respectively. These values of bulk density were arbitrarily selected after reviewing related works[1),23),26)].

3.3 Results and discussion

3.3.1 Soil behavior under cyclic torsional shear loading

When a constant cyclic torque was applied to a soil specimen in the form of sinusoidal pattern, the consequent cyclic torsional shear stress, torsional shear strain, and

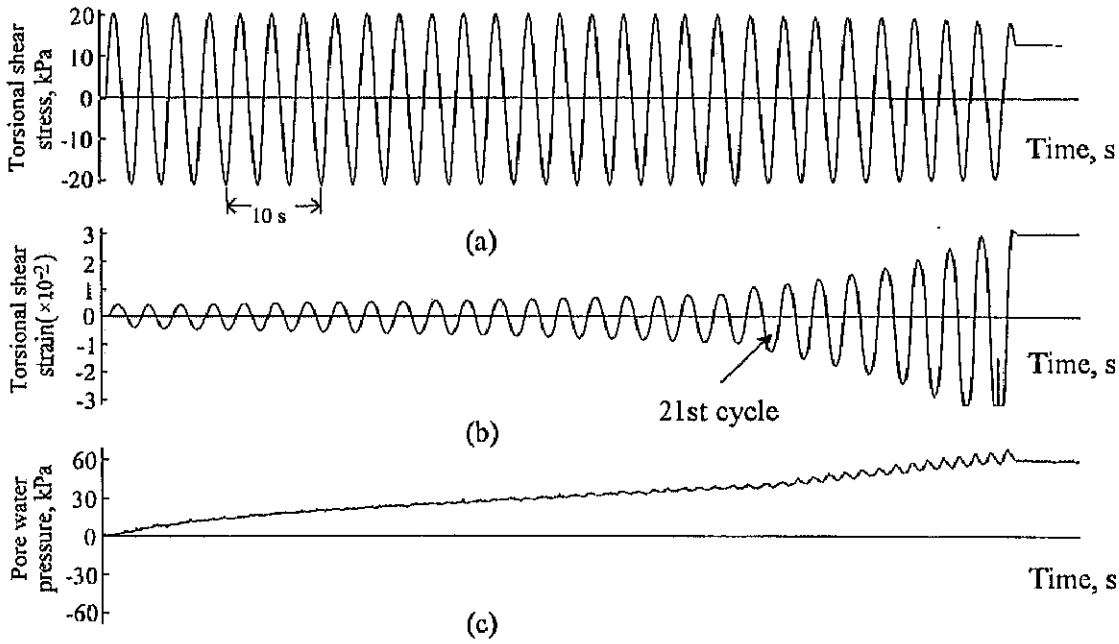

Fig. 3.5 Time histories of (a) torsional shear stress, (b) torsional shear strain and (c) pore water pressure.

pore water pressure were obtained as shown in Fig. 3.5. The torsional shear stress changed sinusoidally corresponding to the applied torsional shear force (Fig. 3.5(a)), while the associated torsional shear strain (Fig. 3.5(b)) showed fluctuation with gradual increase of its amplitude when time lapsed. Moreover, a comparatively large amount of torsional shear strain was observed starting at Nc = 21. The pore water pressure also exhibited a similar

increasing trend as the torsional shear strain (Fig. 3.5(c)). In addition, the amplitude of torsional shear stress started to decrease at Nc = 21 owing to a loss of shear strength.

The significance of the development of pore water pressure exists in decreasing the effective confining stress and leading to the loss of soil strength. This is a specific feature found in the undrained cyclic loading test. Seed[79] stated that during earthquakes, the build-up of pore water pressure occurred due to the cyclic shear stresses that were induced by the ground motion. This is also produced by traffic loads in underlying subgrade soil[44]. Similarly, this phenomenon might be encountered in the field during machinery traffic, especially in mechanized agriculture which heavy machines and intensive passages are involved.

In contractive loose saturated sand, this pore water pressure will increase until reaching a value equal to the applied confining pressure, and the sand will rapidly begin to undergo large deformations afterwards with shear strains exceeding 20% or more. This phenomenon is referred to as liquefaction[79]. On the other hand, in dilative dense sand, the cyclic mobility is normally recognized with the appearance of initial liquefaction and progressive softening of a specimen[16), 17), 79)]. Unlike the above cases, according to results in Fig. 3.5, the strain softening phenomena could be observed in this test after the 21st cycle of loading but initial liquefaction did not occur. However, the pore water pressure was developed up to 30% of the confining pressure at this stage. This may be due to the difference in the physical properties of test soils. A similar characteristic was found to appear in some cases of undrained cyclic loading of clayey soil such as the results of tests performed by Hyodo *et al.*[40] Yasuhara *et al.*[96] stated that clay behavior under undrained cyclic loading is more complex than that of sand behavior. One factor affecting this is content of fine soil particle as reported by Gou and Prakash[32], who studied the effect of

fine content in silt and silt clay on liquefaction. Another possible cause is that this test was a torque control not an actual stress control test. If a stress control test were conducted, the initial liquefaction might have appeared or at least the pore water pressure would have developed up to a higher percentage of the confining pressure.

It seemed that rearrangement of soil particles might have occurred at the initial stage of applying cyclic torsional shear load as indicated by the comparatively rapid increases of pore water pressure during that period (Fig. 3.5(c)). More obvious representation can be provided exhibiting the relationship of the pore water pressure and torsional shear strain in Fig. 3.6. As shown in the figure, development of pore water pressure compared with the increase of torsional shear strain was higher in period-A than period-B. It showed that the greater changes of soil particle structures at the beginning period might occur. Guo and Prakash[32] described that clay content or fine particles imposed a higher increasing rate of pore water pressure because the clay content will

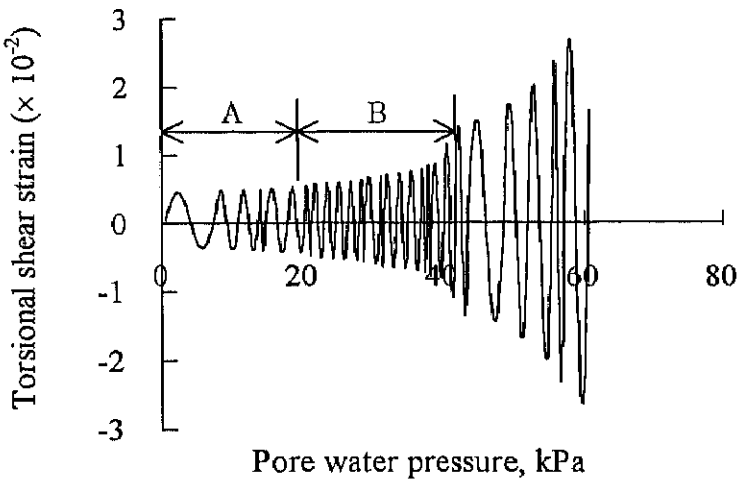

Fig. 3.6 Relationship between torsional shear stress and effective confining stress.

reduce the hydraulic conductivity of the soil. This should also help clarify the rapid rate of pore water pressure during period-A in which more fine particles might be dispersed in pore space. However, after soil particles move to mechanically balanced positions to secure structural stability by their rearrangement, the effect of fine particle might be small and then pore water pressure increased with relatively constant rate during period-B. The record of vertical displacement showed that the soil specimen's height was reduced by about 3.0 mm.

3.3.2 Effect of cyclic torsional shear stress

While more interest is placed on large deformation produced during cyclic loading application in the study of earthquake-induced liquefaction, small deformation, on the other hand, should also be taken into consideration in the study of the traffic-induced field soil compaction. Even a small change of soil properties in the field might affect plant growth[90]. The effect of cyclic torsional shear stress during cyclic loading is expressed in Fig. 3.7. Soil specimens subjected to higher amplitudes of the stress could result in higher amounts of torsional shear strain, especially at higher Nc.

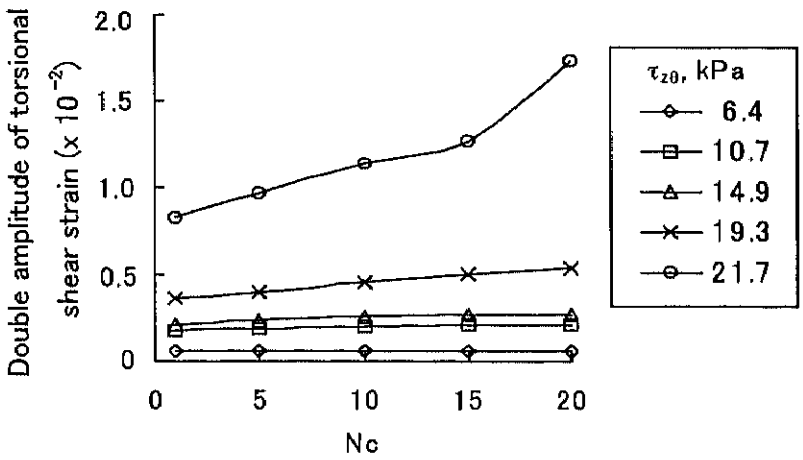

Fig. 3.7 Double amplitude of torsional shear strain versus Nc.

Fig. 3.8 depicts the change of torsional shear strain in relation to cyclic torsional shear stress. The increasing rate of torsional shear strain grew when cyclic torsional shear stress increased. It can be seen that torsional shear strain for Nc = 20 increased about four times when the stress increased from 6 to 20 kPa. However, for further application of the stress, a small increase of stress from 20 to 22 kPa also resulted in the same increment of the strain that was approximately four times higher. This represents the effect of high

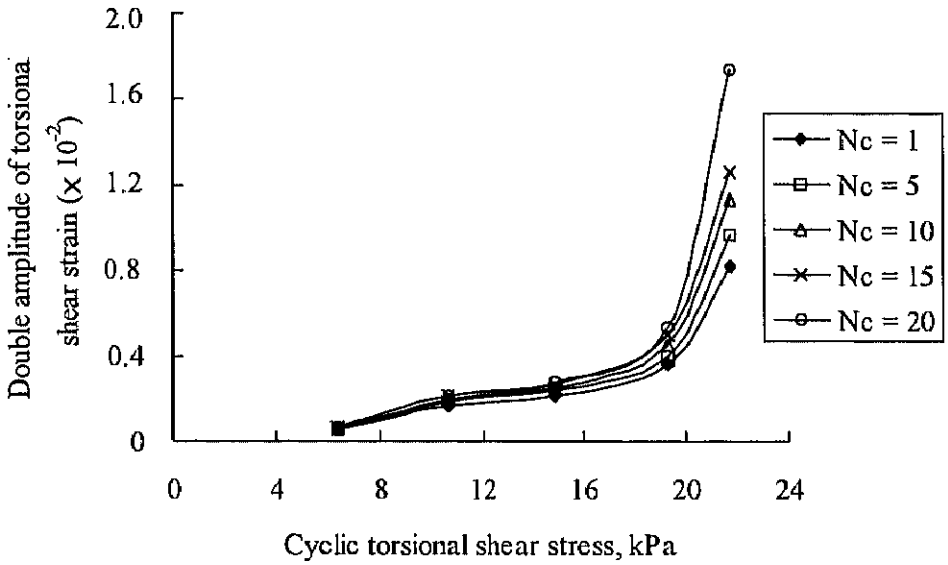

Fig. 3.8 Double amplitude of torsional shear strain versus cyclic torsional shear stress.

cyclic torsional shear stress on corresponding soil deformation and suggests that a critical amount of stress might be of importance. The significance of this critical value exists in contributing to the selection of machine size to use in the field so that soil deformation can be restricted. It should be noted that all of the test results shown in Figs. 3.7 and 3.8 did not encounter the strain softening phenomena even at the highest Nc (Nc = 20). Therefore, the relatively large torsional shear strains appearing in the figures were not caused by the occurrence of strain softening as expressed at the 21st cycle in Fig. 3.5 but loss of soil

strength against cyclic loading.

According to literature review, among the factors affecting soil compaction, the machine weight and the number of passage are instrumental. Their influences were also discussed in this study in relation to torsional shear strain as shown above (Figs. 3.7 and 3.8). In addition, the interrelation between these factors in terms of loading intensity that was reported by some previous field works[45),4),82),94)] was also manifested to some extent. As shown in Fig. 3.9, loading under the condition of $\tau_{z\theta}$ = 19.3 kPa for Nc = 43 and 49 could produce the equivalent amounts of torsional shear strain that were induced by $\tau_{z\theta}$ = 21.7

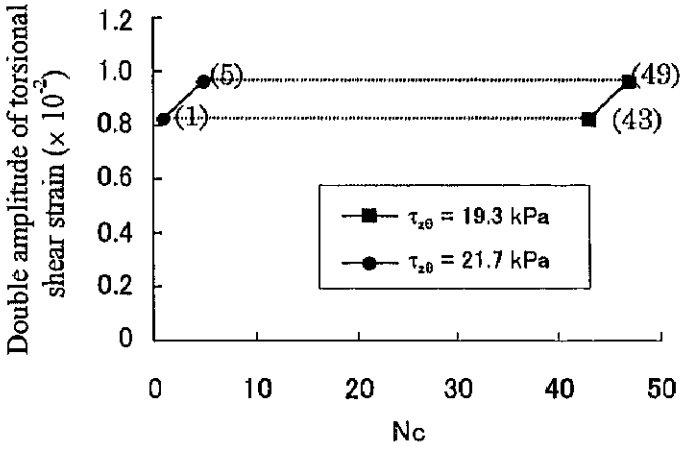

Fig. 3.9 Nc requirement for same double amplitude of torsional shear strain.

kPa at Nc = 1 and 5, respectively. In field tests, it was found that under the same traffic intensity of light and heavy tractor with different numbers of passage could bring about the same soil compaction level[45)]. However, it is of interest to note that the Nc required for $\tau_{z\theta}$ = 19.3 kPa to yield the same amount of the strain that was produced by $\tau_{z\theta}$ = 21.7 kPa at Nc = 1, was rather high. This might be due to the rapid increase of torsional shear strain starting from 20 kPa depending on confining stress as shown in Fig. 3.8. If the comparison is made in the lower region, the required Nc must be smaller.

3.3.3 Effect of loading frequency

In accordance with various settings of the travel speed, corresponding loading frequencies generated by a tractor became different. According to previous works[46], the loading frequencies by the 10 to 50kW class tractor for various operations such as plow tillage, planting operation and fertilizer application were considered, ranging from 0.29 to 1.55 Hz as listed in Table 3.3. Taking into account these actual field situations together with easy testing manipulatability, three different loading frequencies of 0.2, 0.5 and 1.0 Hz were determined for this indoor experiment.

Table 3.3 Loading frequencies induced by traffic during tractor operation in the field

plow tillage	0.74~1.55Hz
rotary tillage	0.29~1.15Hz
planting operation	0.57~1.60Hz
fertilizer application	0.80~1.60Hz
harvesting operation	
forage harvester	0.40~1.03Hz
combine	0.40~0.86Hz

The effects of loading frequency on soil behavior were observed by analyzing the results of torsional shear stress-strain at Nc = 20 in Fig. 3.10. Judging from the figure in the large torsional shear strain region, it can be deduced that the amplitude of torsional shear strain at Nc = 20 took greater values in the order of 1.0, 0.5 and 0.2 Hz. However, its interrelationship with loading frequency in the lower τ_{20} domain is difficult to explain. This may partly be due to the disturbance of intrinsic, unavoidable vibration caused by torque-applying components of the test apparatus.

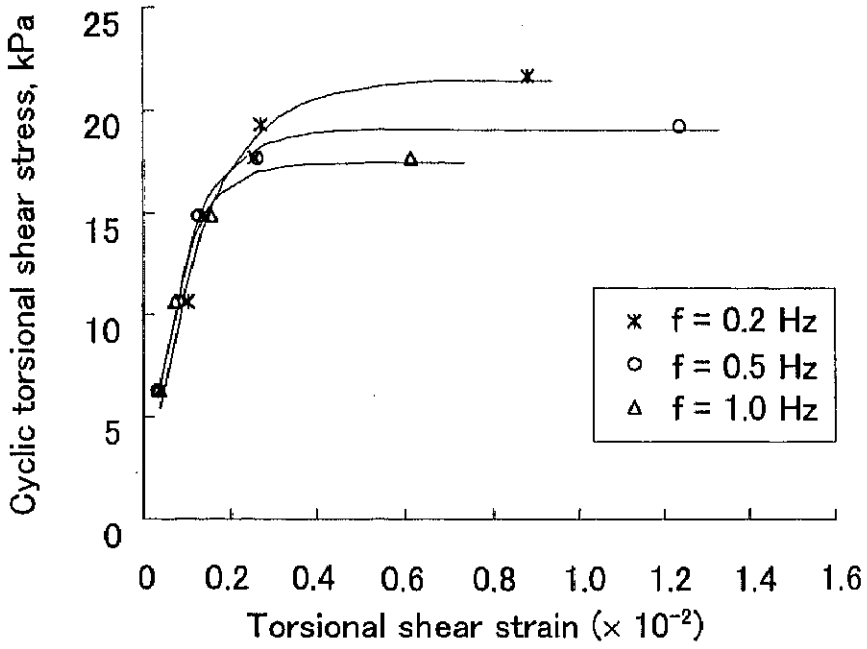

Fig. 3.10 Cyclic torsional shear stress versus torsional shear strain (ρ = 1.0 Mg/m^3, Nc = 20).

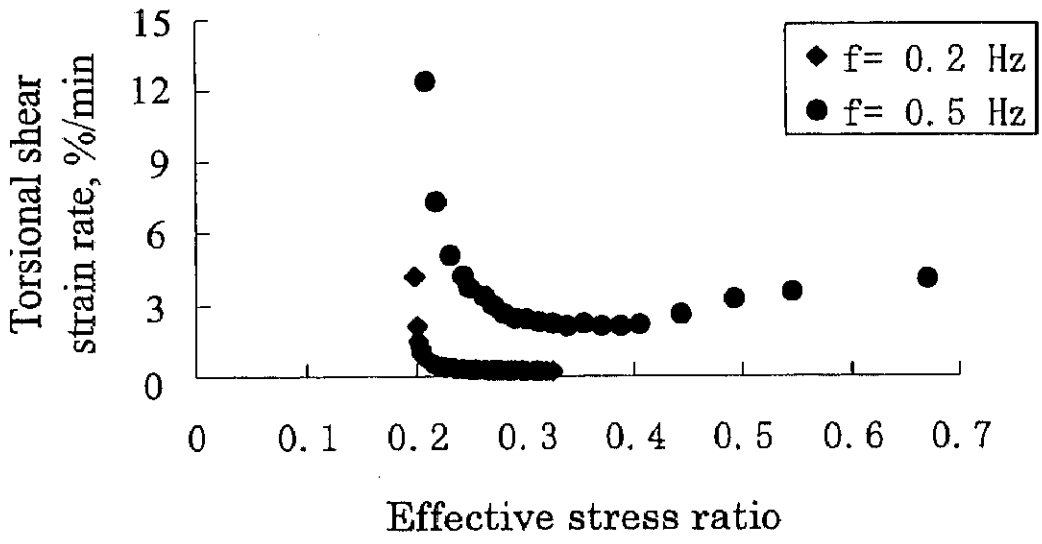

Fig. 3.11 Torsional shear strain rate versus effective stress ratio.

The effect of frequency on torsional shear strain could probably be described as follows. When a soil specimen is subjected to higher loading frequency, the soil particles might be forced to move quicker to the corresponding direction. Hence, the torsional shear strain rate was higher as shown in Fig. 3.11. Consequently, the pore water pressure increased rapidly and had less time to disperse sufficiently within the specimen. As a result, it produced a higher amount of torsional shear strain with successive Nc. The torsional shear strain rate was defined by dividing the amplitude of torsional shear strain by loading time. In fact, the loading frequency of 0.5 Hz must produce a loading rate to soil specimen 2.5 times higher than that of 0.2 Hz. However, it was found that the strain rate created by 0.5 Hz was more than 2.5 times higher. As shown in Fig. 3.11, the strain rate in the loading case of 0.5 Hz was about 5.5 times higher than one of 0.2 Hz. This resulted in a much higher insufficient degree of dispersion of pore water pressure in the loading frequency of 0.5 Hz.

There are some previous reports relating to the effect of frequency on the dynamic behavior of soil. Among these studies, the problematic results are also reported. Zhang[97] conducted cyclic loading tests to investigate strain-rate effects on transient shear strength. Under a high frequency range of 1 to 20 Hz, the axial strains developed were smaller in tests with higher frequency than in tests with a lower frequency. This was due to the more rapidly changing loading direction during the cyclic stress application of higher frequency. A similar result was observed by Koike *et al.*[51] who carried out the cyclic loading test for unsaturated soil specimens. Their results showed that at the stress ratio of 0.1, the amplitude of axial strain for 0.5 Hz excitation became greater than that of 1.0 Hz. In contrast, according to Adebiyi *et al.*[3], the amplitude of axial strain for the frequency of 1.5 Hz was higher than that of 0.5 Hz at the cyclic stress ratio of 0.25. However, they noted

that when the cyclic stress ratio was higher than 0.40 the effect of frequency was difficult to ascertain.

Based on the results of this experiment and literature review, it may be suggested that the effect of frequency on associated strain depends upon specific parameters such as the magnitude of cyclic stress, range of frequency and soil property. At low cyclic stress ratio and high frequency domain, higher frequency seemed to yield lower strain because of the more rapidly changing loading direction during cyclic stress application as mentioned by Zhang[97]. On the other hand, at high cyclic stress ratio and low frequency domain, higher strain can be obtained under higher loading frequency since higher strain rate does not allow enough time for sufficient dispersion of pore water pressure. This weakens soil strength faster and led to larger amplitude of strain at successive Nc. However, the necessity of further tests to prove the above-mentioned should be noted.

3.3.4 Effect of bulk density

The effect of bulk density on cyclic torsional shear loading was discussed in preparation with bulk density of 0.8, 0.9 and 1.0 Mg/m^3. The results of cyclic torsional shear loading at Nc = 20 and frequency of 0.2 Hz are shown in Fig. 3.12.

With more pore space of the soil specimen, or lower bulk density, larger amplitude of torsional shear strain was obtained. The amplitude of torsional shear strain took increasing value in the order of 1.0, 0.9 and 0.8 Mg/m^3. In addition, there was unbalance in the torsional movement of soil particles in specimens having low bulk density, which was frequently found in soil specimens of 0.8 Mg/m^3 in this test as shown in Fig. 3.13. The continuing increase of absolute value of torsional shear strain growed roughly until Nc = 30 and followed steady-state situation afterwards. In this figure, only the early stage of the process was represented for a reference. However, this was not explicitly observed in

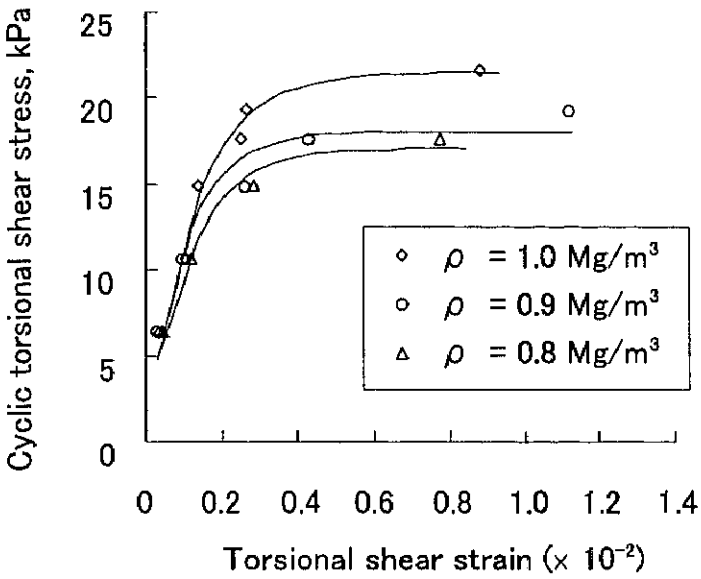

Fig. 3.12 Cyclic torsional shear stress versus torsional shear strain (f = 0.2 Hz, Nc = 20).

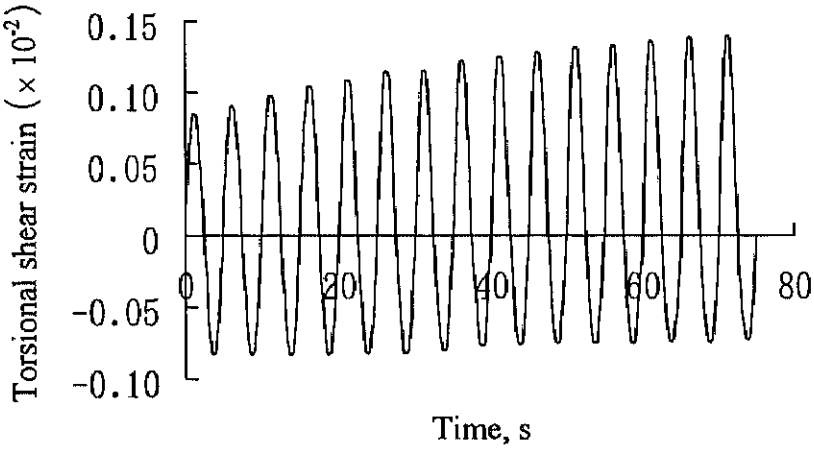

Fig. 3.13 Time history of torsional shear strain (ρ = 0.8 Mg/m³, f = 0.2 Hz).

the case of 1.0 Mg/m^3. This phenomenon seems to appear due to the inhomogeneity of soil specimens that occurs during the process of specimen preparation, which is frequently found in the case of specimens having low bulk density.

3.3.5 Effect of confining stress

When external force is applied to soil, one of the major parameters affecting the change of soil behavior is confining stress. Higher confining stress provides more soil strength against external force. In the field, soil is subjected to a different amount of confining stress along the soil profile due to the weight of the overlying soil layer.

In order to predict the effect of confining stress, the tests were conducted with different levels of confining stress but with a constant cyclic torsional shear stress of 10.7 kPa. The results are shown in Figs. 3.14 and 3.15. It was found that the increase of confining stress reduced the development of torsional shear strain. Besides, it tended to alleviate the effects of bulk density and loading frequency. The different amounts of

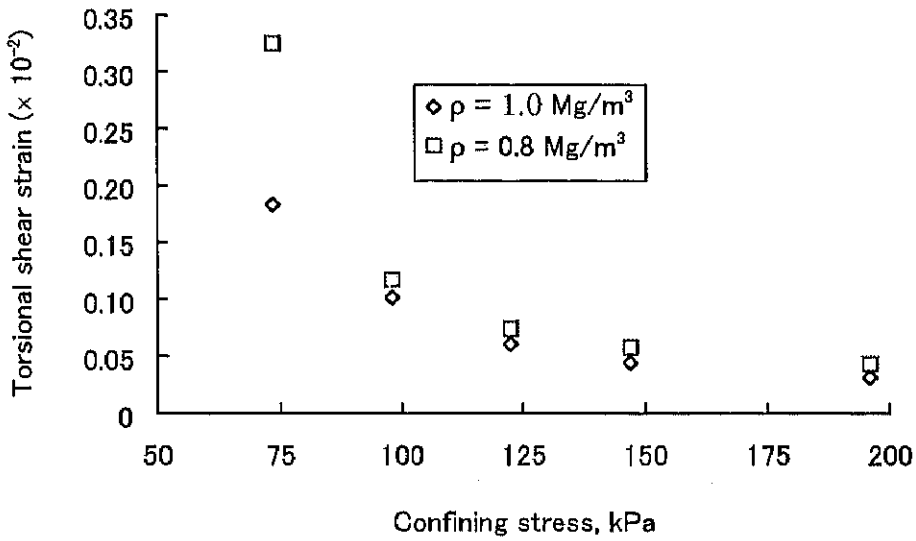

Fig. 3.14 Confining stress versus torsional shear strain (f = 0.2 Hz, Nc = 20).

torsional shear strain that were produced in different bulk densities and by different loading frequencies were big at low confining stress but small at high confining stress, as shown in Figs. 3.14 and 3.15, respectively.

Moreover, since the relations of torsional shear strain and confining stress seemed to exhibit an asymptote parallel to the axis of confining stress, it implies the existence of a

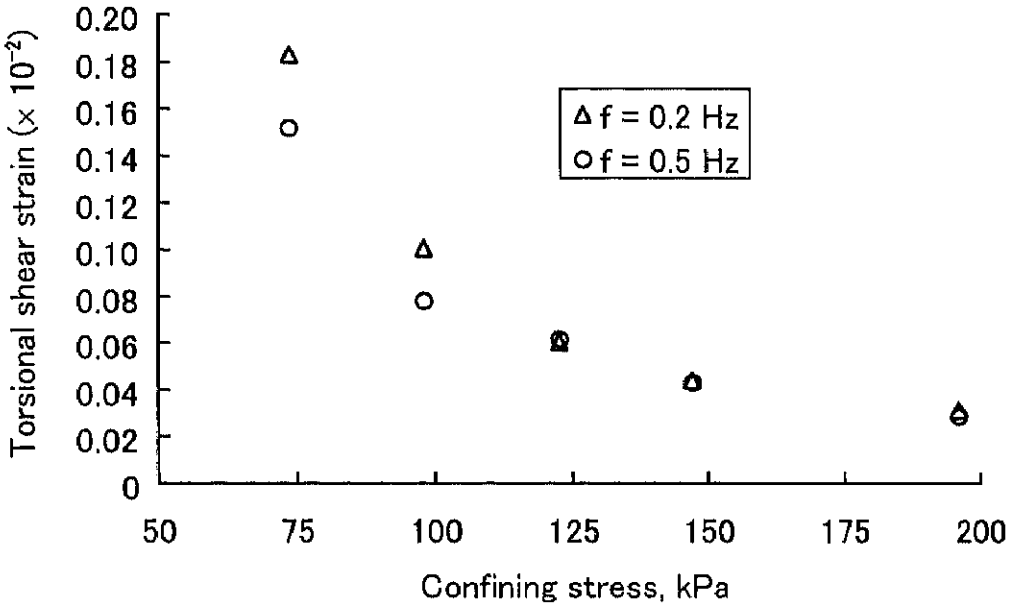

Fig. 3.15 Confining stress versus torsional shear strain (ρ = 1.0 Mg/m^3, Nc = 20).

limiting region of the soil profile being disturbed by external force. When it comes to actual application, this relationship may be useful in the prediction of the stress propagation in the soil profile.

3.3.6 Torsional shear strain and effective stress ratio

The effective stress ratio, $\tau_{z\theta}/\sigma'_c$, is defined as the ratio of amplitude of cyclic torsional shear stress to effective confining stress at the end of each loading cycle. The effective stress ratio serves as an indicator of the stress state on soil without the existence

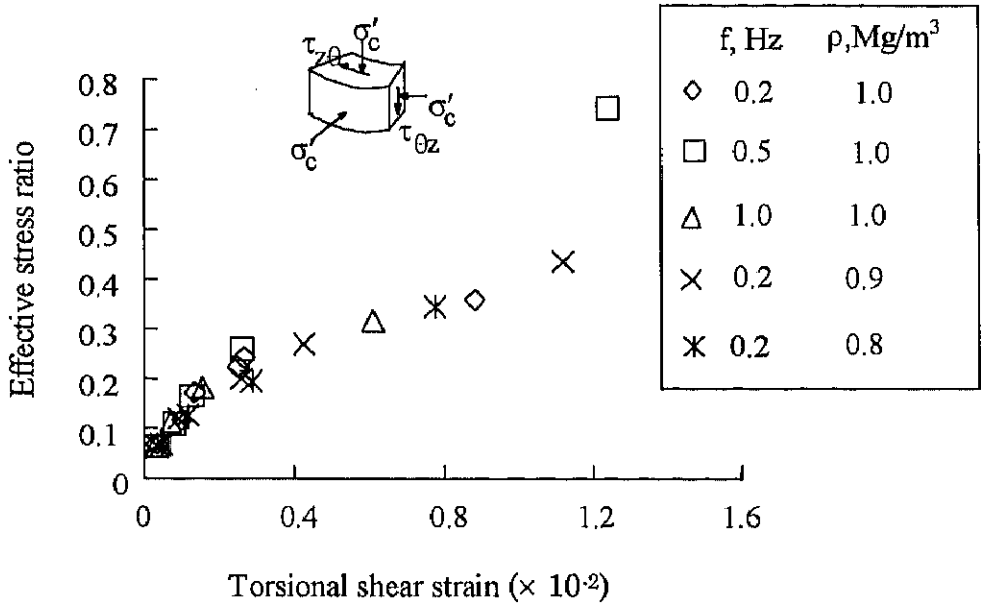

Fig. 3.16 Effective stress ratio versus torsional shear strain at Nc = 20.

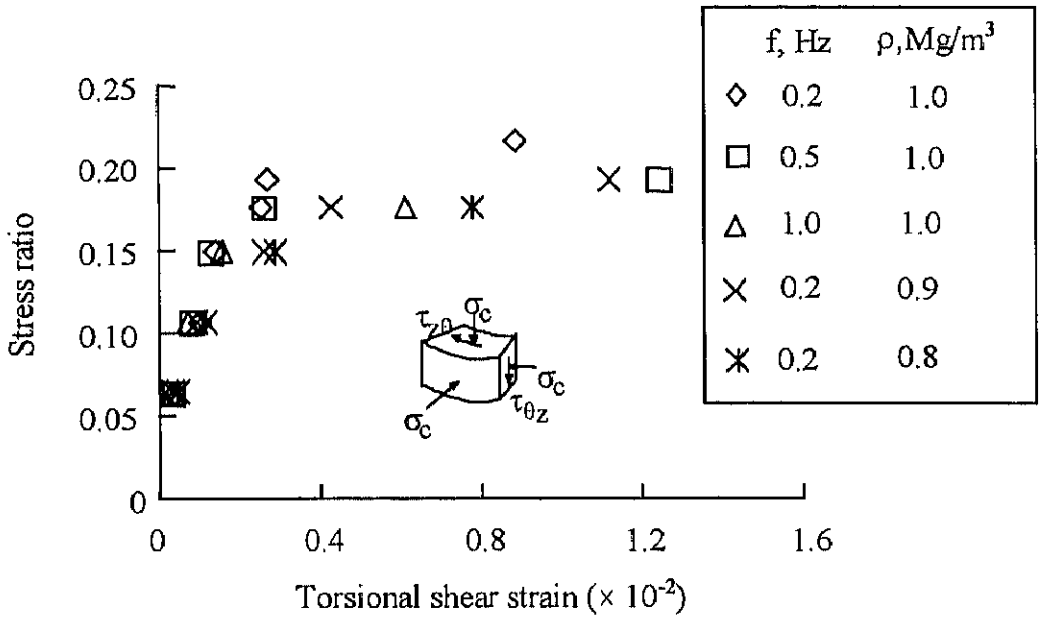

Fig. 3.17 Stress ratio versus torsional shear strain at Nc = 20.

of pore water pressure. Changes of torsional shear strain under experimental combinations listed in the Figs. 3.16 and 3.17 were found to coincide well when plotted against effective stress ratio (Fig. 3.16) whereas they tended to scatter with the stress ratio, $\tau_{z\theta}/\sigma_c$ (Fig. 3.17).

These results indicate that when the effective stress ratio was taken into consideration, the influences of loading frequency and bulk density did not appear, and then the amplitude of cyclic torsional shear strain was found to be unique under an identical effective stress ratio.

3.4 Summary

Indoor experiment tests using the cyclic torsional shear loading test method were conducted to clarify the dynamic behavior of soil compaction induced by repetitive passages of a tractor in the field, particularly focusing on the turning operation. Moreover, the specific needs for field soil compaction were quite different than those for liquefaction. Therefore, the tests were conducted to implement the breakthrough of the essential prediction and explanation for the behavior of field soil compaction. It was ascertained that an increase in terms of the number of cyclic loading caused a continuing increment of both torsional shear strain and pore water pressure until the strain softening phenomena appeared, due mainly to a build-up of pore water pressure. The magnitude of torsional shear strain was affected by loading magnitude, confining pressure, loading frequency and bulk density. However, when the effective stress ratio was taken into consideration, the effect of loading frequency and bulk density did not appear.